Differential Role of Transient Receptor Potential Channels in Ca^{2+} Entry and Proliferation of Prostate Cancer Epithelial Cells

Stephanie Thebault,[1] Matthieu Flourakis,[1] Karine Vanoverberghe,[1] Franck Vandermoere,[2] Morad Roudbaraki,[1] V'yacheslav Lehen'kyi,[1] Christian Slomianny,[1] Benjamin Beck,[1] Pascal Mariot,[1] Jean-Louis Bonnal,[1] Brigitte Mauroy,[1] Yaroslav Shuba,[1] Thierry Capiod,[1] Roman Skryma,[1] and Natalia Prevarskaya[1]

[1]Laboratoire de Physiologie Cellulaire, Institut National de la Sante et de la Recherche Medicale and [2]Laboratoire de Biologie du Développement, Centre National de la Recherche Scientifique, Université des Sciences et Technologies de Lille, Villeneuve d'Ascq, France

Abstract

One major clinical problem with prostate cancer is the cells' ability to survive and proliferate upon androgen withdrawal. Because Ca^{2+} is central to growth control, understanding the mechanisms of Ca^{2+} homeostasis involved in prostate cancer cell proliferation is imperative for new therapeutic strategies. Here, we show that agonist-mediated stimulation of α_1-adrenergic receptors (α_1-AR) promotes proliferation of the primary human prostate cancer epithelial (hPCE) cells by inducing store-independent Ca^{2+} entry and subsequent activation of nuclear factor of activated T cells (NFAT) transcription factor. Such an agonist-induced Ca^{2+} entry (ACE) relied mostly on transient receptor potential canonical 6 (TRPC6) channels, whose silencing by antisense hybrid depletion decreased both hPCE cell proliferation and ACE. In contrast, ACE and related growth arrest associated with purinergic receptors (P2Y-R) stimulation involved neither TRPC6 nor NFAT. Our findings show that α_1-AR signaling requires the coupled activation of TRPC6 channels and NFAT to promote proliferation of hPCE cells and thereby suggest TRPC6 as a novel potential therapeutic target. (Cancer Res 2006; 66(4): 2038-47)

Introduction

After androgen escape, the prostate tumor cell proliferation becomes independent of normal growth control mechanisms. Various growth factors, neurotransmitters, and hormones, known to control physiologic and pathologic cell proliferation, participate in the maintenance of intracellular Ca^{2+} homeostasis. Although the nature of these agonists has yet to be well established during prostate cancer progression, they invariably induce a Ca^{2+} entry called "agonist-induced Ca^{2+} entry" (ACE; refs. 1–4).

Despite α_1-adrenoceptor (α_1-AR) antagonists being already widely used for the clinical treatment of benign prostate hyperplasia (5), the exact role of α_1-AR–coupled signaling pathway in prostate cancer growth control remains unclear. α_1-AR antagonists induce apoptosis in human prostate cancer epithelial (hPCE) and smooth muscle cells without affecting the cellular proliferation (6), independently of their effects on α_1-AR (7, 8). Using an androgen-dependent lymph node carcinoma of the prostate (LNCaP) cell line (9), we have previously shown that α_1-AR stimulation activates nonspecific cationic channels leading to ACE (10).

Interestingly, we have also shown that in contrast to the stimulatory role of α_1-ARs on prostate cancer cell growth, metabotropic purinergic receptors (P2Y-R) are involved in the growth arrest of DU-145 human prostate cancer cells (11). Such divergent effects of two receptors on cell proliferation are surprising, because both α_1-AR and P2Y-R are known to be coupled to the common phospholipase C (PLC)–catalyzed inositol phospholipids breakdown signaling pathway, via which α_1 agonists and extracellular ATP are capable of inducing apparently similar increases in intracellular free Ca^{2+} ($[Ca^{2+}]_i$; refs. 12, 13). The opposite end effects on cell proliferation can only be explained if the ACE controlled by each receptor uses different but still undetermined Ca^{2+}-permeable membrane channels ultimately destined to target various intracellular effectors. Currently, the members of the extensively studied transient receptor potential (TRP) channel family, especially TRP canonical (TRPC) subfamily (14), are considered as the most promising candidates as underlying various types of ACE, including ACE involved in proliferative cell activity (15–18). However, the involvement of TRPs in the mechanisms of translation of generated Ca^{2+} signal into proliferative activity of prostate cancer cells is far from being understood.

The expression of genes involved in cell proliferation and apoptosis is regulated by nuclear transcriptional factors. Nuclear factor of activated T cells (NFAT) proteins represent a family of Ca^{2+}-dependent transcription factors (19) whose activity is regulated by Ca^{2+}/calmodulin–dependent protein phosphatase, calcineurin (19). Another ubiquitously expressed transcription factor is represented by the nuclear factor-κB (NF-κB) family (20), which is known to be dependent on Ca^{2+} homeostasis, especially on the filling status of Ca^{2+} endoplasmic reticulum (ER) stores (14).

In the present study, we asked first whether the divergent effects on prostate cancer epithelial cell proliferation of ACE triggered by distinct membrane receptors via common signaling cascade could be explained by different coupling efficiencies of Ca^{2+} entry pathways involved in either NFAT or NF-κB activation. Second, we wished to ascertain, if the latter were so, what type of membrane channels underlies these pathways. To this end, we used primary cultures of hPCE cells established from resection specimens, which is much more relevant from practical perspectives than using cell lines.

Materials and Methods

Primary culture. Human prostate specimens were mechanically dissociated and then cultivated in KSF medium (Life Technologies Bethesda Research Laboratories, Gaithersburg, MD) supplemented with 50 μg/mL bovine pituitary extract and 50 ng/mL epidermal growth factor to

Note: Y. Shuba is currently at the Bogomoletz Institute of Physiology, National Academy of Sciences of Ukraine, Bogomoletz Street, 4, 01024 Kiev, Ukraine.

M. Flourakis and K. Vanoverberghe contributed equally to this work.

Requests for reprints: Stephanie Thebault, Laboratoire de Physiologie Cellulaire, Institut National de la Sante et de la Recherche Medicale EMI 0228, Bâtiment SN3, Université des Sciences et Technologies de Lille, 59655 Villeneuve d'Ascq Cedex, France. Phone: 33-3-20-43-40-77; E-mail: stephanie_thebault@yahoo.fr.

doi:10.1158/0008-5472.CAN-05-0376

specifically select epithelial cells. Each sample was analyzed by immunofluorescence staining to verify the epithelial marker expression (cytokeratins 14 and 18; ref. 21; data not shown). The culture medium also contained 50,000 IU/L penicillin and 50 mg/L streptomycin. Cells were routinely grown in 50-mL flasks (Nunc, Poly Labo, Strasbourg, France) and kept at 37°C in a humidified incubator in an 95% air/5% CO_2 atmosphere. For electrophysiology and calcium imagery experiments, the cells were subcultured in Petri dishes (Nunc, Naperville, IL) and used after 3 to 6 days. Each primary culture was only maintained for 2 weeks to prevent the lost of their differentiated phenotype.

We used specimens from four localized prostate cancers of Gleason score 8 to 10, prostate-specific antigen (PSA) level of $\geq$4.0 ng/mL, and clinical tumor stage T_2, from patients having undergone a radical prostatectomy, selected on the criteria that the tumors were nonmetastatic, and had no history of chemotherapy and/or antiandrogen therapy. Thus, the prostate cancer epithelial cells derived from the specimens most likely represented androgen-dependent population. The absence of normal epithelial cells was confirmed by independent histologic and anatomopathologic analyses. All experimentations on patients tissues were done according to the medical ethics under the agreement number "CP 01/33" delivered by the "Comité Consultatif de Protection des Personnes dans la Recherche Biomédicale de Lille."

Calcium imaging. $[Ca^{2+}]_i$ was measured using fura-2 (as previously described; refs. 22, 23). The extracellular solution contained 120 mmol/L NaCl, 6 mmol/L KCl, 2 mmol/L $CaCl_2$, 2 mmol/L $MgCl_2$, 10 mmol/L HEPES, and 12 mmol/L glucose. For Ca^{2+}-free HBSS, $CaCl_2$ was removed, and EGTA (0.5 mmol/L) was added.

Electrophysiology and solutions. Whole-cell patch-clamp techniques were used for current recording, as detailed elsewhere (24, 25). The extracellular solution contained 150 mmol/L NMG, 20 mmol/L CsCl or 10 mmol/L $CaCl_2$, 20 mmol/L TEA(Cl) at pH 7.3 (adjusted with HCl). The intracellular solution contained 125 mmol/L NMG, 10 mmol/L HCl, 1 mmol/L $MgCl_2$, 2.6 mmol/L $CaCl_2$ (calculated $[Ca^{2+}]_{free}$ = 100 nmol/L), 10 mmol/L HEPES, 8 mmol/L EGTA, and 20 mmol/L NaCl at pH 7.2 (adjusted with glutamic acid).

Reverse transcription-PCR analysis. Total RNA from the hPCE cells was isolated as previously detailed (10). For the PCR reaction, specific sense and antisense primers were designed, based on Genbank hTRP sequences, using Genejockey II (Biosoft, Cambridge, United Kingdom) as listed in Table 1. To further identify the PCR-amplified products, each PCR band was subjected either to the restriction analysis using the specific enzymes for each amplified fragment or subcloned in TA-cloning vector (Invitrogen, San Diego, CA) followed by the sequencing analysis.

The sequences of selected oligonucleotides used as sense and antisense are presented in Table 1.

Transient transfection. For antisense assays, the sense (control) and antisense oligonucleotides (Eurogentec, Southampton, United Kingdom) targeted against each TRPC (TRPC1, TRPC3, TRPC4, and TRPC6) were designed at the initiating ATG codon level (see Table 1 for sequences). The hPCE cells treated for up to 72 hours with either 0.5 μmol/L phosphorothioate antisense oligodeoxynucleotides and 2.5 μmol/L cytofectin (GS 3815 to DOPE at a 2:1 molar ratio, unsized; Eurogentec) or sense oligodeoxynucleotides by adding them directly to the culture medium. The oligodeoxynucleotides transfection procedures were as detailed previously (26).

Cis-reporting systems (pNFAT-Luc plasmid, pNF-kBLuc plasmid and pCIS/CK negative control plasmid) were provided by Stratagene (Pathdetect In vivo Signal Transduction Pathway *cis*-Reporting Systems, La Jolla, CA). hPCE cells maintained in DMEM-HG were plated in six-well plates overnight and transfected with the *cis*-reporting system selected using Geneporter-2 (Ozyme, Saint-Quentin en Yvelines, France) in 2 mL serum-free DMEM-HG. After 8 hours, 2 mL serum-free media were added, containing either 10 μmol/L phenylephrin or 100 μmol/L ATP (Sigma, St. Louis, MO).

Western blot. TRPC6, cyclin-dependent kinase 4 (cdk4), cdk inhibitor p27 (p27), β-actin, and calnexin protein expression was assayed by Western blot with anti-TRPC6-specific (ACC-017, Alomone, Jerusalem, Israel),

Table 1. Sequences of selected oligonucleotides used as reverse transcription-PCR primers or as sense and antisense

Targets fragment	Oligonucleotides sequences	Position in Genbank sequence (accession no.)	Expected size (bp)
PCR primers			
hTRPC1	Forward: 5′-AGTGGGAACGACTCATCCTTTT-3′	300-322 (NM_003304)	632 (TRPC1)
	Backward: 5′-CATAGTTGTTACGATGAGCAGC-3′	931-910 (NM_003304)	530 (TRPC1A)
hTRPC3	Forward: 5′-CTTCTCTAGGTCCATGGAGGGAA-3′	150-172 (U47050)	417
	Backward: 5′-TCAGAGTGAGACGCTTGCTGGC-3′	568-547 (U47050)	
hTRPC4	Forward1: 5′-GCAGAGACGAAGAAATAGCATGGCA-3′	205-229 (AF063822)	455
	Backward1: 5′-CTGGAGTGAATTCAGAGAACTGCT-3′	659-636 (AF063822)	
hTRPC4	Forward2: 5′-CTCTGGTTGTTCTACTCAACATG-3′	2058-2082 (AF063822)	781 (TRPC4)
	Backward2: 5′-CCTGTTGACGAGCAACTTCTTCT-3′	2861-2839 (AF063822)	528 (TRPC4b)
			356 (TRPC4d)
			332 (TRPC4g)
hTRPC6	Forward1: 5′-TTCCCGCCATGAGCCAC-3′	420-436 (AJ006276)	208
	Backward1: 5′-CGGTGAGCCAGTCTGTTGTCAGAT-3′	627-604 (AJ006276)	
hTRPC6	Forward2: 5′-GAACTTAGCAATGAACTGGCAGT-3′	1322-1345 (AJ006276)	625 (TRPC6)
	Backward2: 5′-CATATCATGCCTATTACCCAGGA-3′	1947-1925 (AJ006276)	461 (TRPC6b)
			277 (TRPC6g)
Actin	Forward: 5′-CAGAGCAAGAGAGGCATCCT-3′	248-267 (NM_001101)	210
	Backward: 5′-GTTGAAGGTCTCAAACATGATC-3′	457-436 (NM_001101)	
Sense and antisense oligonucleotides			
hTRPC1	Antisense: 5′-GCCATCATCGCGGCCCAT-3′	405-388 (NM_003304)	
	Sense: 5′-ATGGGCCGCGATGATGGC-3′	388-405 (NM_003304)	
hTRPC3	Antisense: 5′-CCATGGACCTAGAGAAGC-3′	166-149 (U47050)	
	Sense: 5′-GCTTCTCTAGGTCCATGG-3′	149-166 (U47050)	
hTRPC4	Antisense: 5′-GTAATAGAACTGAGCCAT-3′	236-253 (AF063822)	
	Sense: 5′-ATGGCTCAGTTCTATTAC-3′	253-236 (AF063822)	
hTRPC6	Antisense: 5′-TCTGGCTCATGGCGGGAA-3′	437-420 (AJ006276)	
	Sense: 5′-TTCCCGCCATGAGCCAGA-3′	420-437 (AJ006276)	

anti-cdk4–specific (NCL-cdk4-35 from Novocastra, Newcastle upon Tyne, United Kingdom), anti-p27–specific (sc-1641 from Santa Cruz Technology, Santa Cruz, CA), anti-β-actin–specific (Lab Vision Co., Fremont, CA), and anti-calnexin–specific (SPA-860, Stressgen, Victoria, British Columbia, Canada) antibodies, as previously described (25). Quantification of the band intensity was done by densitometry on Quantity-One software (Bio-Rad, Hercules, CA). For each experiment, the signal intensity obtained for TRPC6, cdk4, and p27 were normalized to calnexin or β-actin value, as loading control.

Immunofluorescence staining. cdk4 and cdk inhibitor p27 expression was assessed by immunofluorescence staining with cdk4 (NCL-cdk4-35 from Novocastra) and p27 (sc-1641 from Santa Cruz Technology) antibodies as previously described (10).

Luciferase assay. The cultures were harvested for luciferase activities 48 hours after transfection. After cell lysis, the level of extracted luciferase from these cells was determined by bioluminescence measurement (Biocounter M1500 luminometer, Lumac, Landgraaf, the Netherlands) using the Luciferase Assay kit (Kit Galacto-Light, Tropix).

Proliferation assays. The CellTiter 96 AQueous Non-Radioactive Cell Proliferation Assay (Promega Corp., Madison, WI) was used to determine the number of viable cells in proliferation as previously described (10). Cells were seeded at an initial density of 7.5×10^3 per well in 96-well plates (Poly Labo). After 48 hours of treatment or growth in control conditions, cells were trypsinized, transferred to separate tubes, and centrifuged at 350 $\times$ *g* for 10 minutes. Each well in the 96-well plate was carefully inspected in the microscope to make sure that all cells were recovered. The supernatant after centrifugation was poured off; the cells were carefully suspended and counted in a Malassez chamber.

Data analysis. Each experiment was repeated several times, and the results were expressed as mean ± SE where appropriate. Data analysis was done by using Origin 5.0 software (Microcal, Northampton, MA).

Results

α_1-AR- and P2Y-R–coupled Ca^{2+} signaling involves different types of Ca^{2+} entry pathways in hPCE cells. Both α_1-adrenergic and P2Y-purinergic receptors are known to stimulate PLC-catalyzed inositol phospholipids breakdown, resulting in the derivation of two secondary messengers important for Ca^{2+} signaling: inositol trisphosphate (IP_3) and diacylglycerol (DAG). IP_3 releases Ca^{2+} from intracellular stores, and the concomitant store depletion activates Ca^{2+} influx via store-operated Ca^{2+} channels (SOC), whereas DAG induces Ca^{2+} entry by directly gating some cationic Ca^{2+}-permeable membrane channels. Interplay among various sources of Ca^{2+} largely determines the profile of intracellular Ca^{2+} concentration.

We first sought to examine the specifics of $[Ca^{2+}]_i$ signals elicited by the stimulation of each receptor in hPCE cells. This was done based on fluorimetric $[Ca^{2+}]_i$ measurements on hPCE cells loaded with Ca^{2+} indicator fura-2AM in response to the bath applications of an α_1-specific agonist, phenylephrine, or a purinergic receptor agonist, ATP.

Figure 1*A* shows that phenylephrine (10 μmol/L) elicited regular slow intracellular Ca^{2+} oscillations. The quantification of the amplitude and temporal variables of these oscillations (n = 67 cells) provided the Ca^{2+} wave peak value of 512 ± 43 nmol/L, the average wave duration of 2.18 ± 0.13 minutes, and the average period of wave generation of 4.2 ± 1.06 minutes. Phenylephrine-evoked $[Ca^{2+}]_i$ oscillations were strictly dependent on extracellular Ca^{2+} ($[Ca^{2+}]_{out}$) completely vanishing upon its withdrawal (Fig. 1*A*), thereby suggesting the absolute requirement of Ca^{2+} influx across the plasma membrane for their support. Moreover, first time

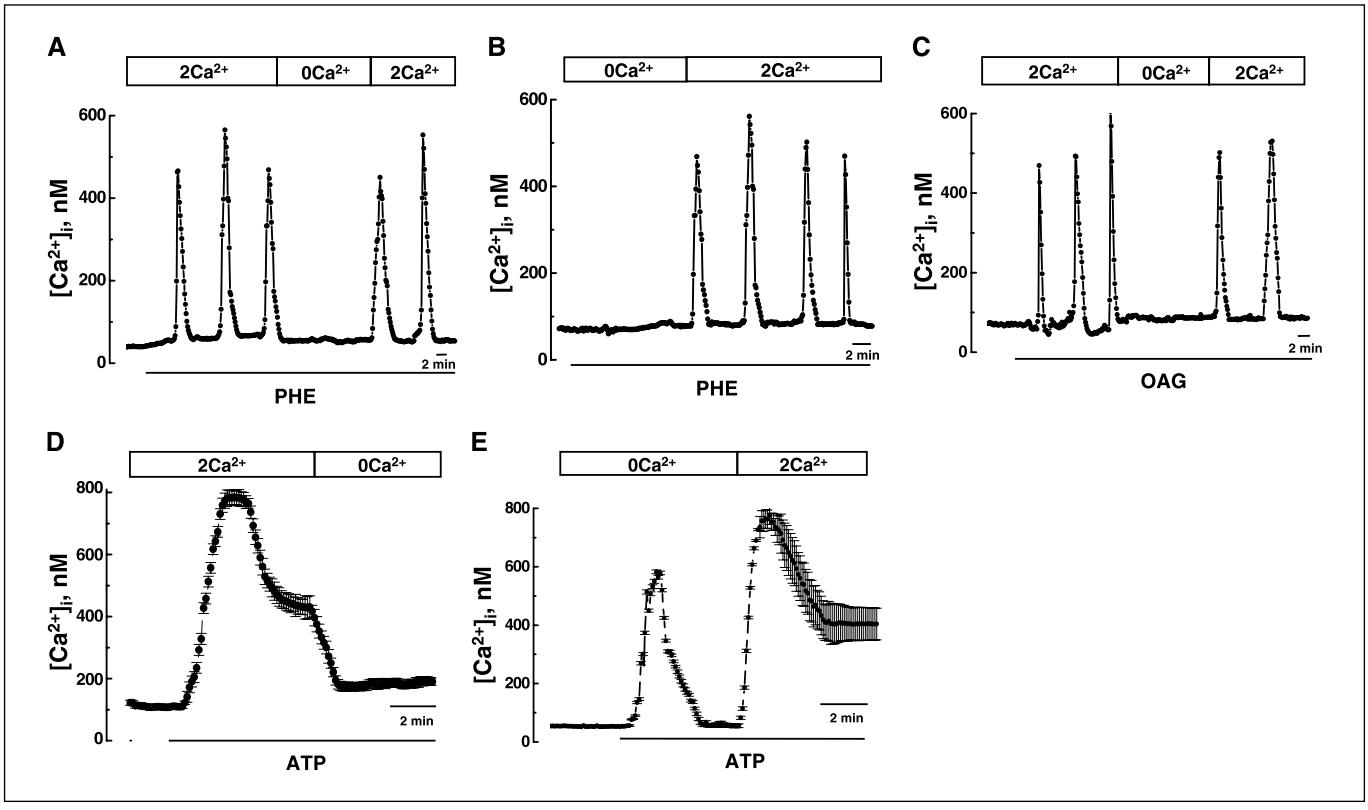

Figure 1. α_1-AR– and P2Y-purinoreceptor–mediated Ca^{2+} signaling in primary hPCE cells. *A* and *B,* patterns of $[Ca^{2+}]_i$ induced by α_1-AR agonist phenylephrine (*PHE*, 10 μmol/L) in hPCE cells initially maintained either in 2 mmol/L (*A, 2/Ca*$^{2+}$, n = 67) or 0 mmol/L (*B, 0/Ca*$^{2+}$, n = 98) extracellular Ca^{2+} and their sensitivity to the subsequent $[Ca^{2+}]_{out}$ variations. *C,* pattern of $[Ca^{2+}]_i$ induced by the membrane-permeable DAG analogue OAG (100 μmol/L, n = 79) in hPCE cells maintained at 2 mmol/L $[Ca^{2+}]_{out}$ (*2/Ca*$^{2+}$) and its sensitivity to extracellular Ca^{2+} removal (*0/Ca*$^{2+}$). *D* and *E,* patterns of $[Ca^{2+}]_i$ induced by P2Y-R agonist ATP (100 μmol/L) in hPCE cells initially maintained either in 2 mmol/L (*D, 2/Ca*$^{2+}$, n = 93) or 0 mmol/L (*E, 0/Ca*$^{2+}$, n = 64) $[Ca^{2+}]_{out}$ and their sensitivity to the subsequent $[Ca^{2+}]_{out}$ variations. *Points,* means; *bars,* SE. All interventions are marked by horizontal bars.

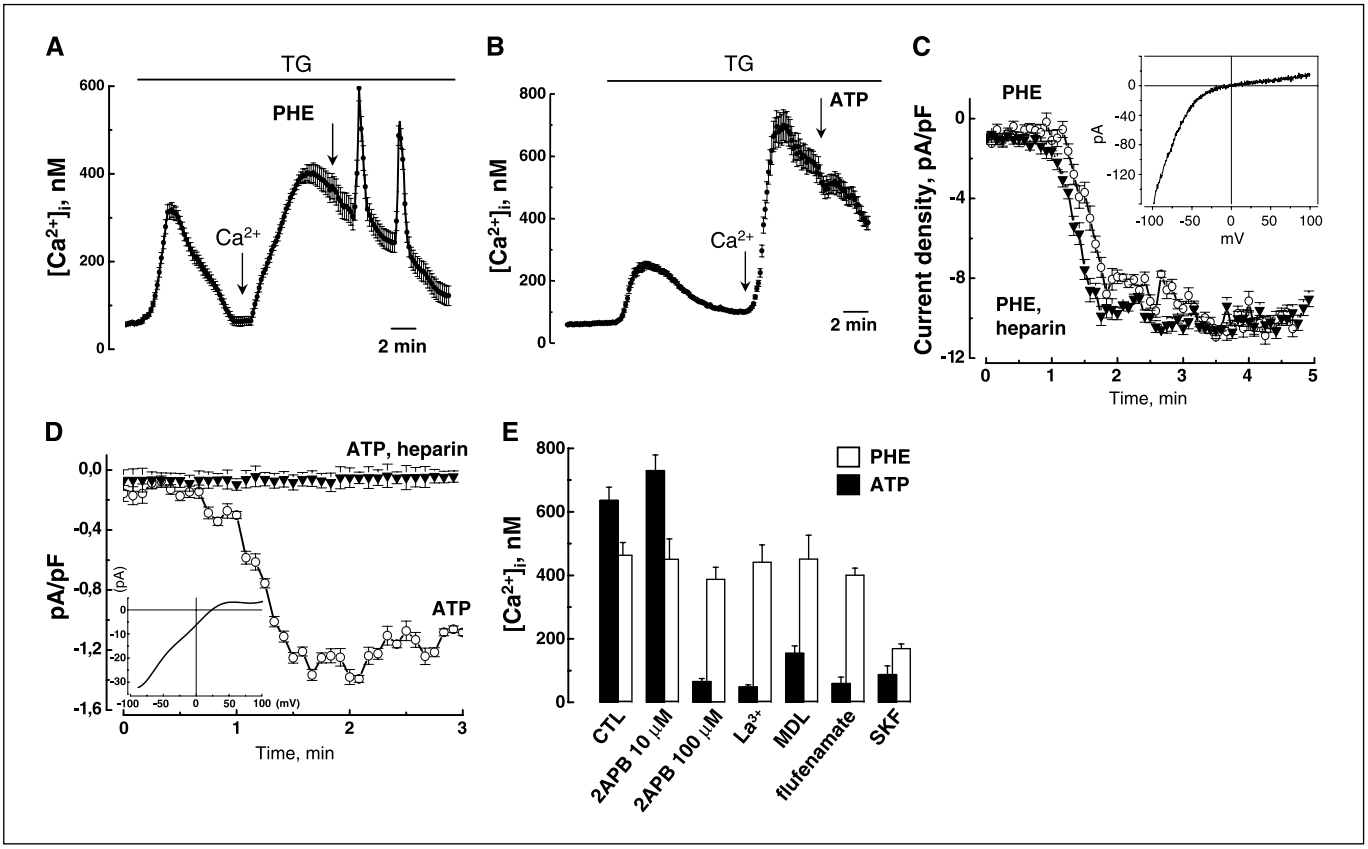

Figure 2. Differential store-dependency of α_1-AR– and P2Y-R–mediated responses in the primary hPCE cells. *A* and *B,* $[Ca^{2+}]_i$ changes in response to hPCE cell exposure to thapsigargin (*TG*, 1 μmol/L) showing Ca^{2+} liberation under 0 mmol/L $[Ca^{2+}]_{out}$ (*0/Ca*$^{2+}$) followed by SOCE upon addition of 2 mmol/L $[Ca^{2+}]_{out}$ (*2/Ca*$^{2+}$) and the ability of phenylephrine (*PHE*, 10 μmol/L, *n* = 61, *A*) but not ATP (100 μmol/L, *n* = 63, *B*) to evoke characteristic $[Ca^{2+}]_i$ signal on top of thapsigargin-induced SOCE. *Points,* mean [*n* = 61 (*A*) and *n* = 63 (*B*)]; *bars,* SE. *C* and *D,* averaged time courses of the inward whole-cell membrane currents activated by phenylephrine (10 μmol/L, *C*) and ATP (10 μmol/L, *D*) in hPCE cells under control conditions (*open symbols* in *C* and *D*) and following the cell's predialysis with IP_3-receptor antagonist heparin (0.1 g/L, *filled symbols* in *C* and *D*) via patch pipette. Currents were measured at membrane potential −100 mV and related to the cells' capacitance to yield current density (pA/pF) before averaging. *I/V* relationships of phenylephrine and ATP-evoked currents (*inset, C* and *D*). *Points,* means (*n* = 5-11); *bars,* SE. *E,* quantification of the effects of common cationic channels inhibitors, 2-APB (10 and 100 μmol/L), La^{3+} (1 mmol/L), MDL (100 μmol/L), flufenamate (50 μmol/L), and SK&F 96365 (SKF, 10 μmol/L), on the amplitude of phenylephrine-induced $[Ca^{2+}]_i$ oscillations (*white columns*) and ATP-induced SOCE (*black columns*) in hPCE cells. *Columns,* means (*n* = 95-102); *bars,* SE.

phenylephrine application in Ca^{2+}-free solution did not cause the mobilization of intracellularly stored Ca^{2+} (Fig. 1*B*; *n* = 98), hence indicating the poor accessibility of IP_3-dependent stores for α_1-AR–triggered signaling and pointing to DAG as a major messenger in this signaling pathway.

Consistent with this notion and in a full agreement with our previous studies (10, 27), the application of 1-oleoyl-2-acetyl-*sn*-glycerol (OAG, 100 μmol/L), a membrane-permeable DAG analogue, exactly mimicked phenylephrine action in terms of inducing $[Ca^{2+}]_{out}$-dependent $[Ca^{2+}]_i$ oscillations (Fig. 1*C*). OAG-induced oscillations even had the same amplitude (546 ± 39 nmol/L, *n* = 79), duration (1.81 ± 0.22 minutes), and period (3.1 ± 0.9 minutes) as the phenylephrine-induced ones, suggesting common mechanisms downstream from DAG and basically ruling out any essential involvement in the IP_3-dependent processes.

In contrast to these observations, ATP (100 μmol/L) evoked a large transient $[Ca^{2+}]_i$ increase (763 ± 25 nmol/L, *n* = 93) followed by a sustained plateau on a considerably lower level, which was sensitive to extracellular Ca^{2+} removal (Fig. 1*D*). Initially administered in the Ca^{2+}-free solution, ATP caused only a transient $[Ca^{2+}]_i$ elevation of 580 ± 28 nmol/L (*n* = 64) without a plateau, as one would expect for pure intracellular Ca^{2+} mobilization (Fig. 1*E*). The reintroduction of Ca^{2+} in the continuing presence of ATP produced a rapid $[Ca^{2+}]_i$ increase followed by a slow decline (Fig. 1*E*), probably reflecting the Ca^{2+}-dependent inactivation mechanism of underlying membrane Ca^{2+} influx channels. Thus, experiments with ATP provide clear evidence for the contribution of both Ca^{2+} release and Ca^{2+} entry in overall $[Ca^{2+}]_i$ and suggest that P2Y-R–controlled Ca^{2+} signaling mostly recruits IP_3- and store-dependent processes in hPCE cells.

Altogether, the results strongly suggest that Ca^{2+} entry pathways participating in α_1-AR–mediated signaling rely on store-independent DAG-gated membrane channels, whereas P2Y-R–mediated signaling engages plasma membrane SOCs, which are activated upon IP_3-dependent Ca^{2+} store depletion.

Differential store dependency of phenylephrine- and ATP-stimulated ACE. To obtain more direct evidence of the differing store dependency and origin of Ca^{2+} entry pathways involved in α_1-AR– and P2Y-R–mediated signaling, we used several approaches. In the first one, we tested for phenylephrine and ATP effects on the background of the ER Ca^{2+} store depletion produced by thapsigargin, a known store-depleting agent acting via inhibition of SERCA-pump Ca^{2+} uptake. In the second, we examined the effect of IP_3 receptor inhibition by heparin on the ability of phenylephrine and ATP to activate membrane currents. Finally, we screened a

number of blockers of various types of native cationic channels and TRP members on their ability to inhibit phenylephrine- and ATP-induced $[Ca^{2+}]_i$ responses.

In the experiments with thapsigargin, we applied it first in Ca^{2+}-free solution to liberate intracellularly stored Ca^{2+} and then we readded Ca^{2+} to initiate store-operated Ca^{2+} entry (SOCE). As Fig. 2*A* shows, if phenylephrine was applied during thapsigargin-induced SOCE, it was still able to activate characteristic Ca^{2+} oscillations on top of SOCE ($n = 61$). In contrast, the same type of ATP application failed to produce any change in $[Ca^{2+}]_i$ on top of thapsigargin-induced SOCE (Fig. 2*B*; $n = 63$).

The inclusion of the IP_3 receptor antagonist heparin (0.1 g/L) in the intracellular pipette solution used in the whole-cell, patch-clamp experiments did not affect phenylephrine-induced membrane current (Fig. 2*C*) but totally abrogated ATP-evoked current (Fig. 2*D*; $n = 5$-11). Phenylephrine and ATP both activated inwardly rectifying membrane currents: *I-V* relationships for both currents are presented in *inset* of Fig. 2*C* and *D*. Phenylephrine-evoked current reached its full amplitude in about 2.0 ± 0.7 minutes, and its average density was 11 ± 1.5 pA/pF at $V_m = -100$ mV ($n = 11$), whereas the average density of ATP-induced current, which reached its full amplitude in about 1.5 ± 0.8 minutes, was 1.3 ± 0.6 pA/pF at $V_m = -100$ mV ($n = 5$).

We also compared the effects of such widely used inhibitors of store-dependent and store-independent membrane Ca^{2+} transport as 2-aminoethoxydiphenyl borate (2-APB), La^{3+}, MDL, flufenamate, and SK&F 96365 on phenylephrine- and ATP-induced Ca^{2+} entry. Given that none of the drugs used was able to affect the temporal variables of phenylephrine-induced $[Ca^{2+}]_i$ oscillations, their effectiveness was evaluated on the basis of their ability to reduce either the amplitude of oscillations in the event of phenylephrine or maximal $[Ca^{2+}]_i$ elevation following Ca^{2+} readdition in the event of ATP. As shown in Fig. 2*E* (n = 95-102), all agents except for 2-APB at low (10 μmol/L) concentration strongly inhibited the ATP-induced response. They exerted virtually no effect on the phenylephrine-induced one except for the SK&F 96365, which blocked the response to phenylephrine by about 50%. Such divergent sensitivity is again consistent with the substantial role played by store-dependent processes in ATP actions but not in those of phenylephrine, because all the agents used are generally known to be more specific to store-operated channels than to other types of cationic channels. Moreover, although 2-APB effects can block both IP_3 receptors and SOCs (28), its ability to stimulate ATP response at a low concentration (10 μmol/L) and to inhibit it at a high concentration (100 μmol/L) agrees closely with the known dual, potentiation inhibition 2-APB action on SOCs (28).

Thus, our results unequivocally show that in hPCE cells, ATP-stimulated P2Y-R–coupled Ca^{2+} signaling involves Ca^{2+} entry via store-operated membrane channels, whereas phenylephrine-stimulated α_1-AR–coupled Ca^{2+} signaling involves Ca^{2+} entry via store-independent DAG-gated Ca^{2+} permeable cationic channels.

TRPC channel expression in hPCE cells. To define the molecular identity of the channels underlying phenylephrine- and ATP-induced ACE, using specific primers (Table 1) and the reverse transcription-PCR technique, we first studied the expression of the mRNA of the human isoforms of the TRPCs (TRPC1, TRPC3,

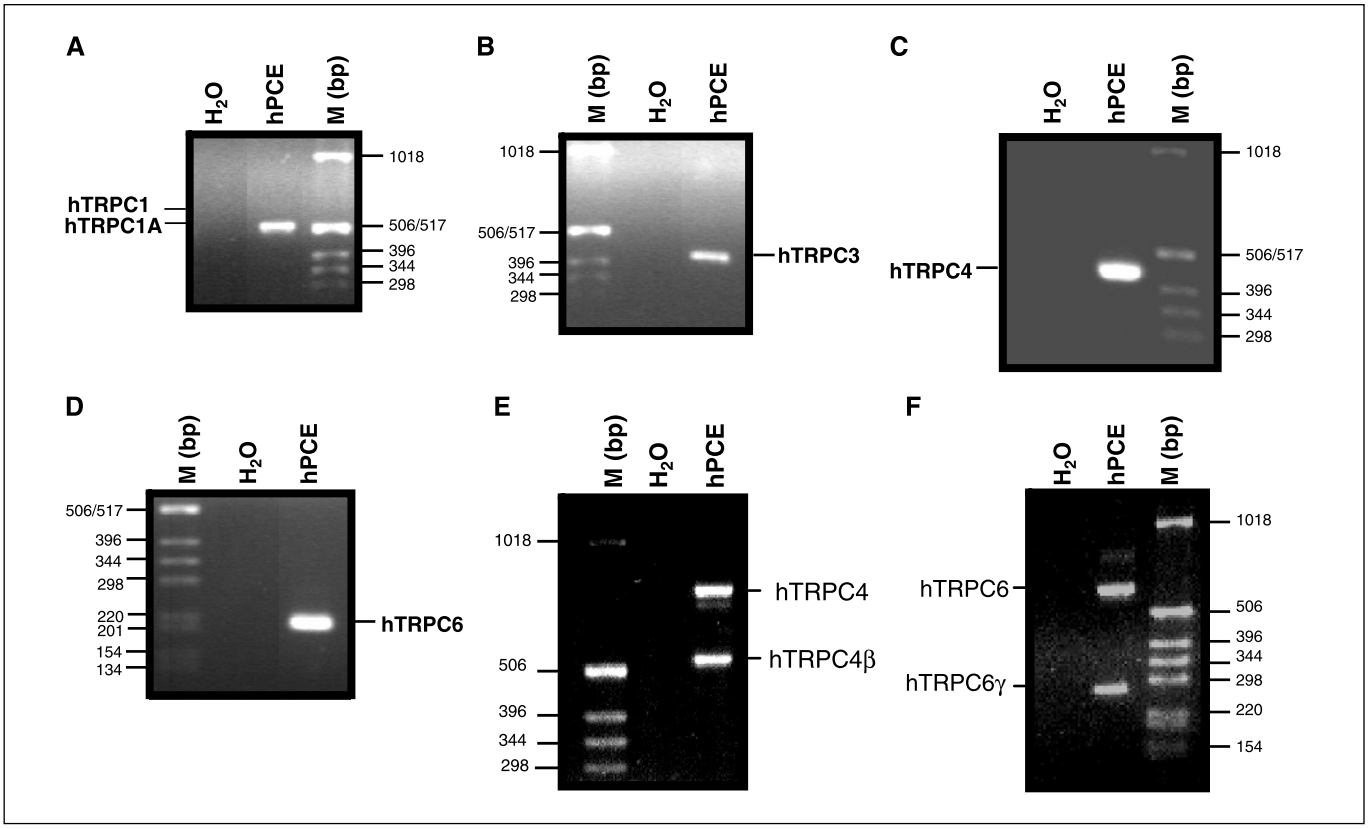

Figure 3. Reverse transcription-PCR analysis of the expression of human TRPC1A (*A*), TRPC3 (*B*), TRPC4 (*C*), and TRPC6 (*D*) transcripts and of human splice variants of TRPC4 (*E*) and TRPC6 (*F*) transcripts in hPCE cells. The expression products were obtained using the primers described in Materials and Methods. *M,* DNA ladder.

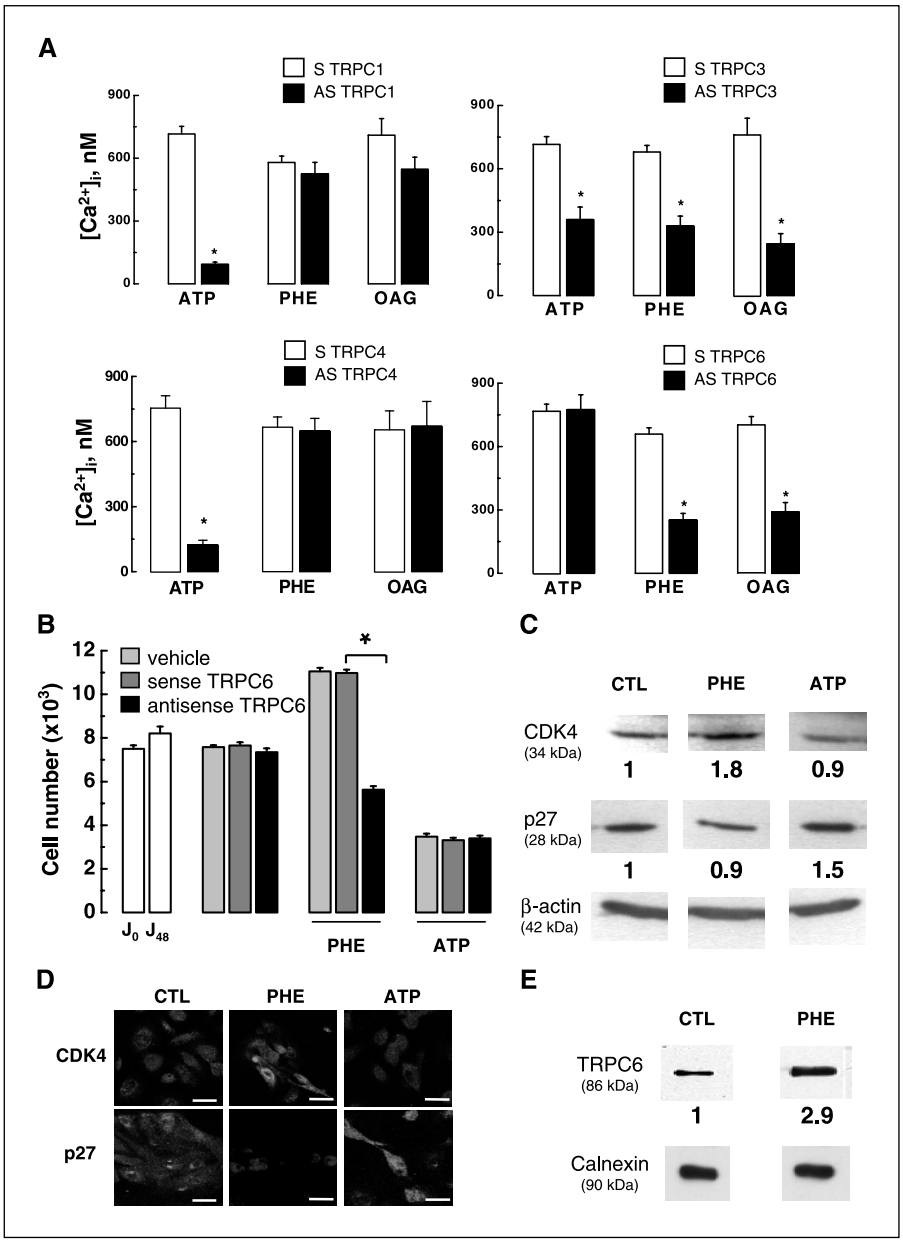

Figure 4. TRPC6 is an important determinant in phenylephrine-induced $[Ca^{2+}]_i$ response and in proliferation-promoting effects of α_1-AR stimulation in hPCE cells. *A,* quantification of $[Ca^{2+}]_i$ signals (see text for details) induced by ATP (100 μmol/L), phenylephrine (*PHE*, 10 μmol/L), and 100 μmol/L OAG in hPCE cells treated for 48 hours with sense (*white columns*) or antisense (*black columns*) oligonucleotides directed against TRPC1 (*top left; n* = 48-85), TRPC3 (*top right; n* = 54-87), TRPC4 (*bottom left; n* = 72-105), or TRPC6 (*bottom right; n* = 59-69). *Columns,* means; *bars,* SE. *, $P < 0.01$. *B,* changes in the density of vehicle-treated hPCE cells (*light gray columns*) and hPCE cells treated with either TRPC6 sense (*dark gray columns*) or TRPC6 antisense (*black columns*) oligonucleotides following 48 hours of incubation under control conditions (*CTL*) and in the presence of phenylephrine (10 μmol/L, *gray column*) or ATP (100 μmol/L, *black column*). *, $P < 0.001$, significantly different values. J_0 corresponds to the initial cell density and J_{48} to the cell density after 48 hours in culture under regular conditions; cells treated with the transfection reagent alone (vehicle) served as control for oligonucleotide treatments. *C,* Western blotting analysis for the expression of cdk4, p27, and β-actin proteins in hPCE cells following 48 hours of culturing in the presence of phenylephrine (10 μmol/L), ATP (100 μmol/L), or in control conditions. *D,* representative epifluorescence images of hPCE cells labeled with FITC-conjugated anti-CDK_4 (*top*) and anti-p27 (*bottom*) antibodies under control conditions and following 48 hours of culturing in the presence of phenylephrine (10 μmol/L) or ATP (100 μmol/L). Bar, 10 μm. *E,* Western blot analysis for the expression TRPC6 protein in hPCE cells following 48 hours of incubation under control conditions or in the presence of phenylephrine (10 μmol/L). Each experiment was repeated thrice.

TRPC4, and TRPC6) in hPCE cells. In the first set of experiments, the specific primers were designed to amplify a portion of the NH_2-terminal sequence surrounding the initiating codon ATG of each TRPC member (Fig. 3*A* and *D*). In the second set of experiments, specific primers were designed to identify the TRPC4 and TRPC6 splice variants isoforms (Fig. 3*E* and *F*), except for the TRPC1 where the NH_2-terminal primers allow us to identify the splice variants. Figure 3 shows the expression of the transcripts for the TRPC1A splice variant (Fig. 3*A*), and the PCR products of the expected sizes for the TRPC3 (Fig. 3*B*), TRPC4 (Fig. 3*C*), and TRPC6 (Fig. 3*D*) in hPCE cells. The study of the splice variants isoforms (Fig. 3*E* and *F*) shows that the TRPC4β and TRPC6γ spliced isoforms were expressed in hPCE cells in addition to unspliced forms of TRPC4 and TRPC6.

Effects of targeted TRPC1, TRPC3, TRPC4, and TRPC6 hybrid depletion on ACE. To elucidate the contribution of each of the identified TRPC members to α_1-AR– and P2Y-R–mediated Ca^{2+} signaling, we employed antisense hybrid depletion technology. We thereby reduced TRPC1/3/4/6 expression, allowing the subsequent evaluation of their effect on phenylephrine-, OAG-, and ATP-stimulated Ca^{2+} influx. We treated the cells with antisense oligonucleotides specific to each TRPC member before using them for Ca^{2+} imaging. Cells treated for the same period of time with respective sense oligonucleotides, which are not supposed to affect endogenous mRNA levels, served as a control. We have previously shown the reduction of specific TRPC1, TRPC3, TRPC4, and TRPC6 mRNA expression in antisense versus sense treated cells by Western blotting analysis in prostate cell line (29, 30).

Because of the oscillatory nature of phenylephrine- and OAG-induced $[Ca^{2+}]_i$ responses and the possibility that altered TRPC expression may potentially affect the amplitude as well as the temporal variables of oscillations, we opted to characterize the resulting effects of antisense treatments by calculating the area under oscillations (i.e., calculating an integral) over the 30-minutes

observation period (S_{Ca}) and then subtracting the $[Ca^{2+}]_i$ baseline. For the phenylephrine-induced oscillations in nontreated hPCE cells under standard conditions, S_{Ca} = 2,700 ± 210 nmol/L . min. In the event of ATP responses, the effects of TRPC depletion was evaluated based on the changes of maximal $[Ca^{2+}]_i$ during the transition from Ca^{2+}-free to Ca^{2+}-containing solution (see Fig. 1*E*).

Figure 4*A* shows that antisense hybrid depletion of TRPC1 (*top left; n* = 48-85) as well as of TRPC4 (*bottom left; n* = 72-105) exerted a pronounced down-regulatory effect on ATP-induced response (i.e., 87% and 84% inhibition, respectively) virtually without affecting phenylephrine- and OAG-induced ones. On the contrary, the antisense knockout of TRPC6 strongly inhibited responses to phenylephrine and OAG (i.e., by 62% and 59%, respectively) leaving the ATP one intact (*bottom right; n* = 59-99). Finally, TRPC3 hybrid depletion affected ATP-, phenylephrine-, and OAG-induced responses almost equally, inhibiting them by 50%, 52%, and 68%, respectively (*top right; n* = 54-87).

Thus, these data indicate that endogenous TRPC1 and TRPC4 channels are exclusively involved in ATP-stimulated store-dependent type Ca^{2+} entry, whereas TRPC6 is the DAG-gated channel mediating phenylephrine-stimulated, store-independent Ca^{2+} entry in hPCE cells. Endogenous TRPC3 is probably plays an equal role in both store-dependent and store-independent Ca^{2+} influx pathways.

α_1-AR agonist phenylephrine but not ATP promotes hPCE cell proliferation via TRPC6 up-regulation. In our previous studies, we have shown that phenylephrine promotes the proliferation of androgen-dependent prostate cancer LNCaP cells via the mechanism involving Ca^{2+} influx (10, 11), whereas extracellular ATP causes the growth arrest of androgen-independent prostate cancer DU-145, by affecting store-dependent processes (10, 11). Therefore, it was natural to examine how the two agonists influence the proliferation of primary hPCE cells as well.

Consistent with our observations of other prostate cancer cell types, 2-day treatments of primary hPCE cells with phenylephrine (10 μmol/L) enhanced their proliferation by 37.3 ± 2.0%, whereas the same period of ATP (100 μmol/L) treatment inhibited cell proliferation by 61.6 ± 1.6% (Fig. 4*B*). To prove the critical involvement of TRPC6 in growth-regulating properties of α_1-AR and P2Y-R agonists, we used hPCE cells subjected to TRPC6 hybrid depletion. In the absence of agonists, TRPC6 sense (TRPC6/s) or antisense (TRPC6/as) oligonucleotides treatment did not modify hPCE cell proliferation activity (Fig. 4*B*). However, in the presence of phenylephrine, the proliferation of TRPC6 sense- and antisense-treated cells becomes dramatically different: if sense treatment did not change the usual proliferation-promoting effects of phenylephrine, then antisense treatment not only abolished these effects but even reversed the trend, consequently resulting in proliferation inhibition. At the same time, TRPC6 sense or antisense treatments did not influence the inhibitory action of ATP on hPCE cell proliferation.

Specific effect of the agonists on cell's proliferation was further confirmed by assaying the expression of two cell cycle regulators, cdk4 and cdk inhibitor p27 (31), by semiquantitative Western blot analysis with anti-cdk4 and anti-p27 antibodies. Inspection of the images presented in Fig. 4*C* shows that phenylephrine treatment resulted in the up-regulation of cdk4 expression and down-regulation of p27 expression in contrast to ATP, whose action on the expression of these cell cycle regulators was exactly opposite. These results were confirmed by immunostaining with FITC-conjugated anti-cdk4 and anti-p27 antibodies (Fig. 4*D*). These data permitted us to conclude that the effects of phenylephrine and ATP on cell count were indeed related to cell proliferation and growth arrest, respectively.

Moreover, semiquantitative Western blot analysis for possible changes in the expression of TRPC6 involved in phenylephrine-induced Ca^{2+} signaling, which is likely to underlie growth-regulating effects, have revealed a ~3-fold up-regulation of TRPC6 expression in response to phenylephrine treatment (Fig. 4*E*).

Altogether, these results point to the key role of TRPC6 in phenylephrine growth-regulating functions.

Proliferation-promoting effects of α_1-AR agonists involve NFAT activation. To determine which transcription factor(s) mediate opposing effects of α_1-AR and P2Y-R agonists on primary hPCE cell growth, we used cells transiently transfected with the pCIS-CK plasmid containing an insert of luciferase reporter gene driven by either synthetic NFAT- or NF-κB–dependent promoter (see Materials and Methods).

Figure 5*A* shows that a 2-day treatment with phenylephrine (10 μmol/L) increased NFAT-dependent luciferase expression by ~5-fold compared with the transfected hPCE cells maintained under control conditions, whereas the same period of ATP (100 μmol/L) treatment did not alter NFAT-dependent luciferase expression, which remained identical to control values. At the same time, neither agonist produced a significant change in NF-κB–dependent luciferase expression (Fig. 5*B*). Moreover, phenylephrine-induced increase in cell proliferation was specifically related to the increased NFAT activity, as blocking calcineurin by cyclosporin A (100 nmol/L) or FK506 (10 μmol/L), thereby impeding nuclear NFAT translocation, prevented the ability of phenylephrine to induce cell proliferation without affecting the ATP-induced growth arrest (Fig. 5*C*). Thus, α_1-AR–mediated stimulation of hPCE cell proliferation mainly occurs via NFAT activation.

Discussion

In the present work, we report three major findings on Ca^{2+} signaling involved in the opposing effects on hPCE cell proliferation of α_1-AR and P2Y-purinergic receptor agonists: (*a*) α_1-AR agonist, phenylephrine, stimulates intracellular Ca^{2+} oscillations sustained by Ca^{2+} entry via store-independent DAG-gated membrane channels predominantly represented by TRPC6, whereas P2Y-R agonist, ATP, stimulates store-dependent and transient Ca^{2+} signal involving SOC activation, to which the major contributors are TRPC1 and TRPC4. (*b*) TRPC6 is a key determinant in proliferation-promoting effects of α_1-AR agonists via oscillatory-type Ca^{2+} signaling. (*c*) α_1-AR agonist–stimulated Ca^{2+} oscillations enhances the coupling efficiency to nuclear Ca^{2+}-dependent transcription factor, NFAT, involved in the activation of proliferation-promoting gene expression.

Agonist-dependent growth regulation of hPCE cells. In this study, we confirmed that the major conclusions regarding the growth-regulating properties of α_1-AR and P2Y-R signaling systems reached in our previous works on model systems of prostate cancel cell lines (10, 11) apply to the primary hPCE cells as well. Our study is the first of its kind to be conducted on primary cells, and its results allow all data, including those obtained in cell lines, to be taken into consideration from a common perspective. This is of importance in view of the widespread usage of cell lines due to their convenience and accessibility, although for practical applications primary hPCE cells represent the preferred model for such studies (for details, see Materials and Methods).

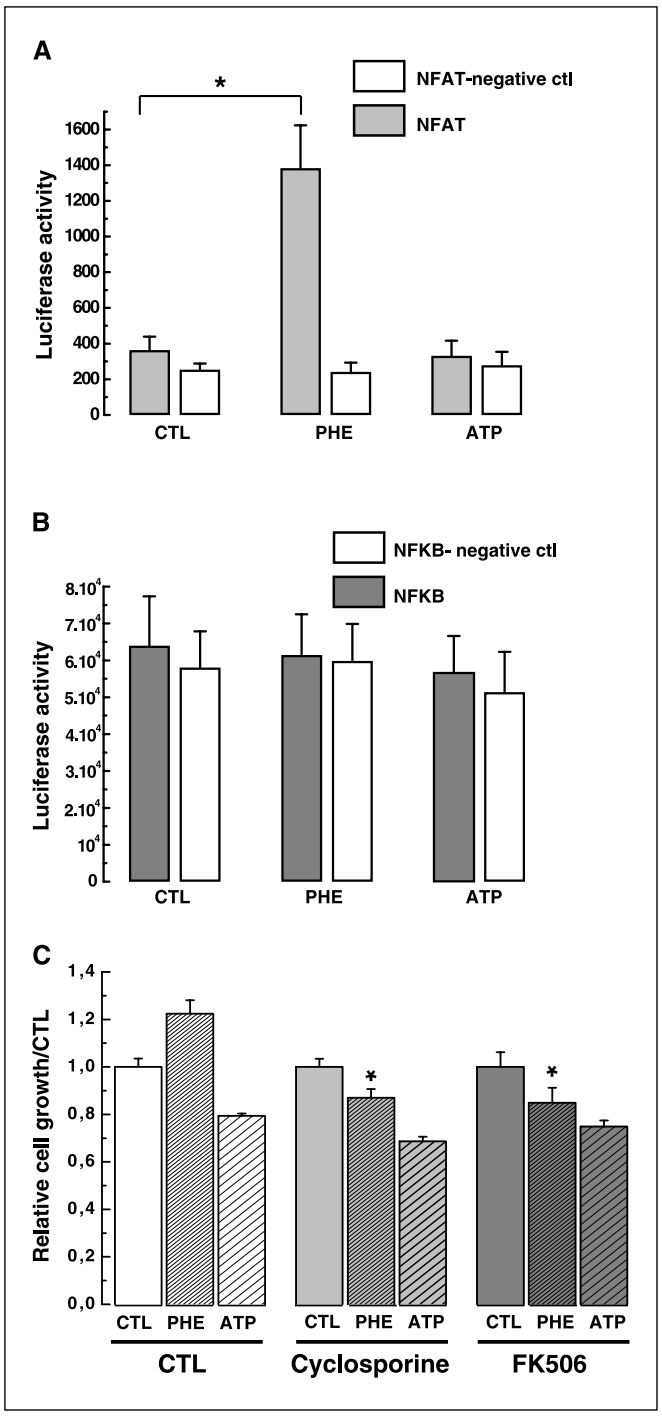

Figure 5. α_1-AR-mediated proliferation-promoting effects involve NFAT activation in hPCE cells. *A,* quantification of luciferase activity in hPCE cells transiently transfected either with a luciferase reporter gene with a NFAT-dependent promoter (*gray columns*) or with a reporter vector lacking NFAT response elements in the promoter (*white columns*) following 48 hours of incubation under control conditions (*CTL*) and in the presence of phenylephrine (*PHE*, 10 μmol/L) or ATP (100 μmol/L). *Columns,* mean of three independent experiments; *bars,* SE. *, $P < 0.01$. *B,* same as in (*A*), but for hPCE cells transiently transfected with a luciferase reporter gene with (*gray columns*) or without (*white columns*) NF-κB–dependent promoter. *C,* changes in the density of hPCE cells in response to 48-hour-long treatment with phenylephrine (10 μmol/L) or ATP (100 μmol/L) under regular (control, *CTL*) conditions and in the presence of calcineurin inhibitors, cyclosporine A (100 nmol/L), or FK506 (10 μmol/L). *, $P < 0.001$, compared with phenylephrine-treated cells under control conditions.

Thus, it seems to be proven that α_1-AR–coupled signaling is associated with the enhancement of hPCE cell proliferation, whereas P2Y-R signaling induces a cessation of proliferative activity. We have shown that despite being initiated by the common PLC-catalyzed inositol phospholipid breakdown, the downstream pathways for the two receptors diverge by preferentially relying on the two different secondary messengers (i.e., IP_3 or DAG). Such a divergence permits the generation of the two different patterns of intracellular Ca^{2+} signal in response to agonist-mediated stimulation of the two receptors, which ultimately result in opposite end effects on cell proliferation.

We show that the pattern of Ca^{2+} signaling initiated by α_1-AR stimulation is characterized by regular oscillatory activity, which is almost exclusively based on Ca^{2+} entry pathway directly gated by DAG with no apparent role for IP_3-mediated store depletion. The latter is shown by the inability of phenylephrine to produce measurable Ca^{2+} release in the absence of extracellular Ca^{2+}. Generally, this is surprising as most models of Ca^{2+} wave generation involve interplay between Ca^{2+} entry and IP_3-mediated, store-dependent processes (25, 26). It may therefore suggest either very localized and compartmentalized Ca^{2+} releases incapable of changing global $[Ca^{2+}]_i$ or the involvement of store-independent Ca^{2+} uptake/extrusion mechanisms, such as, for instance, a mitochondrial one. In contrast, Ca^{2+} signaling coupled to P2Y-R stimulation is largely determined by IP_3-mediated, store-dependent processes, including robust Ca^{2+} release and the activation of store-operated Ca^{2+} influx (Fig. 6). Currently, it is well known that IP_3 has a short half-life within the cell, and that the diffusion of locally produced IP_3 is rate limiting (32–34). However, little is known about assessing these variables in single cell: there are rather used computational models, but no indicator is available that would allow IP_3 to be visualized (35). Similar difficulties seem to study the intracellular signaling of DAG. The carbon-11–labeled DAG was proposed to evaluate its intracellular signaling, but its use needs further investigations (36). Due to these technical limitations, addressing the question of such divergence between α_1-AR–coupled and P2Y-R signaling seems unrealistic.

Recent data suggest that oscillatory $[Ca^{2+}]_i$ activity may be especially suited to the specificity of Ca^{2+} signaling (37), as the possibility of amplitude and frequency signal encoding permits distinct effectors to be targeted. Our data on selective proliferation promoting α_1 agonist action via the induction of Ca^{2+} oscillation in hPCE cells are consistent with this notion. Moreover, the fact that these oscillations translate into enhanced hPCE cell proliferation, via the activation of the Ca^{2+}-dependent transcription factor, NFAT, generally agrees with previous findings on the importance of Ca^{2+} signal amplitude and frequency characteristics, in determining the efficiency and specificity of coupling to various transcription factors, including NFAT (37). In contrast, Mignen et al. have reported that repetitive Ca^{2+} oscillations due to low agonist concentration could not enhance the Ca^{2+}-dependent activation of NFAT in m3-HEK293, whereas high agonist concentration that induced a sustained elevation in cytosolic Ca^{2+} concentration was able to translocate NFAT (38). However, the Ca^{2+} signal pattern was markedly different in their experiments: the Ca^{2+} concentrations were elevated for only a few seconds ($\sim$10-15) during each oscillation (39), whereas the oscillatory period in T cells and in hPCE cells was $\sim$2 minutes.

On the other hand, the antiproliferative effect of ATP-mediated P2Y-purinergic receptor stimulation, via the induction of store-dependent Ca^{2+} signaling, are generally consistent with the critical

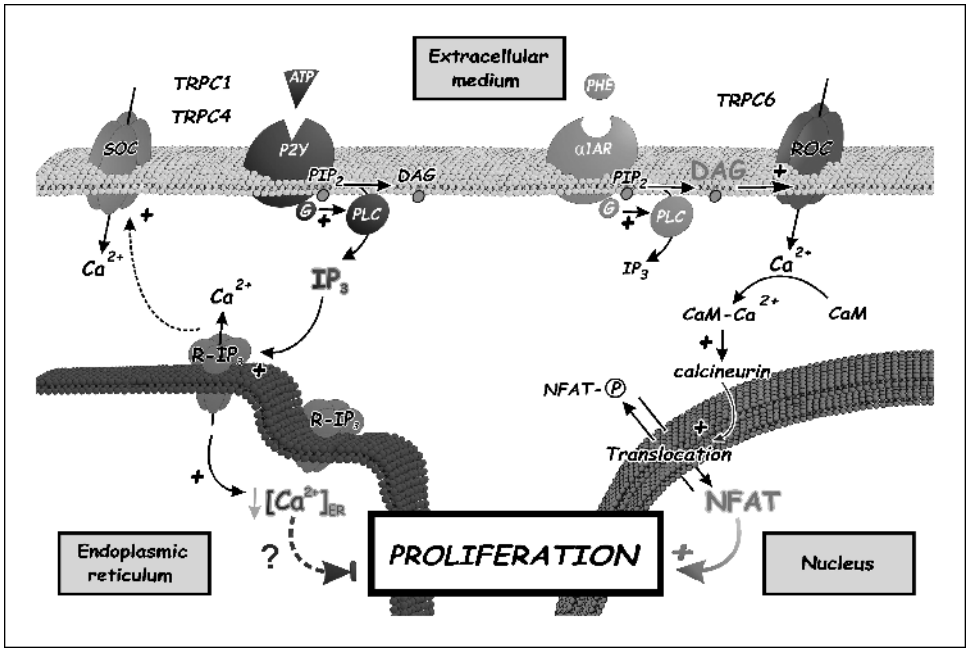

Figure 6. Schematic depiction of α_1-AR– and P2Y-purinoreceptor–mediated Ca^{2+} signaling in the primary hPCE cell proliferation. α_1-AR stimulation by agonist (phenylephrine, *PHE*) via G-protein–coupled PLC-catalyzed PIP_2 breakdown causes generation of two secondary messengers, IP_3 and DAG, of which DAG directly activates the plasma membrane receptor-operated channel (*ROC*) represented by TRPC6, whereas IP_3 due to some limitations of a yet unknown nature, is unable to produce visible effects. Consequent Ca^{2+} entry via ROC/TRPC6 causes NFAT activation due to Ca^{2+}/CaM/calcineurin–assisted translocation to the nucleus, where NFAT initiates the expression of the genes necessary for proliferation. In contrast, agonist-mediated P2Y-R stimulation (ATP), although causing the same PLC-catalyzed derivation of IP_3 and DAG, further down employs IP_3 to release Ca^{2+} from ER via IP_3 receptor (*IP_3-R*) with the subsequent activation of plasma membrane SOC, mainly represented by TRPC1 and TRPC4. Associated ER Ca^{2+} store depletion most probably serves as a primary stress factor for proliferation inhibition.

role of the ER Ca^{2+} store content and SOCs in the regulation of prostate cancer cell apoptosis, as shown in our previous works (23, 25). Indeed, persistent activation of P2Y-purinergic receptors may cause chronic underfilling of ER Ca^{2+} store and an adaptive decrease in SOCE, which although may not be sufficient to induce apoptosis (23, 25), but sufficient to exert antiproliferative effects (11).

TRP members involved in agonist-stimulated Ca^{2+} entry in hPCE cells. Our results also highlight the importance of Ca^{2+} entry pathways in the discrimination of the signaling via α_1-adrenergic and P2Y-purinergic receptors in hPCE cells. Indeed, the α_1-AR agonists, phenylephrine, as well as the DAG analogue, OAG, activate Ca^{2+} entry mainly via the TRPC6 channel, whereas ATP-evoked Ca^{2+} entry predominantly involves TRPC1 and TRPC4 channels.

The literature ascribing various TRPC members to the DAG-gated or SOC type and their mode of activation is quite conflicting and controversial (40–42). Therefore, a thorough assessment of the contribution of each particular TRP in the creation of the specific type of Ca^{2+} entry pathway is required in every case. Thus far, our own data on LNCaP cell line only suggests that TRPC1 and the member of the "vanilloid" TRP subfamily, TRPV6, are predominantly involved in SOC formation (26), which agrees closely with the TRPC1 role in ATP-induced store-dependent type Ca^{2+} entry established above. Moreover, TRPC1 is one of those channels most involved in store-operated Ca^{2+} entry in general (40). Another TRPC member, TRPC4, which we also identified as essentially contributing to ATP-induced, store-dependent type Ca^{2+} entry in hPCE cells, has been shown both in the SOCE and in other cell models (41).

Although the existence of a direct DAG-gated activation mode for heterologously expressed TRPC6 is well established (42–44), our study is the first to identify endogenous TRPC6 as a primary determinant in physiologically relevant agonist-induced Ca^{2+} entry operating on the direct DAG gating mechanism in cells of prostate origin. Moreover, we not only uncover the TRPC6 involvement in the generation of phenylephrine-induced Ca^{2+} oscillations in hPCE cells but also show the likely role of this channel in the enhancement of the pro-proliferative effects of α_1-AR agonists, because chronic exposure to phenylephrine causes TRPC6 overexpression. It is also quite plausible that promotion of proliferation in response to α_1-ARs stimulation may result not only from the higher coupling efficiency of Ca^{2+} oscillations to NFAT activation but also from the spatial colocalization of TRPC6 with the machinery of Ca^{2+}-dependent NFAT activation.

In general, the role of TRP members in proliferation activity has been best studied for smooth muscle cells. Interestingly, the results of these studies point to both TRPC1 and TRPC6 as important determinants in the promotion of pulmonary vascular smooth muscle cell proliferation (45, 46). However, the underlying mechanisms seem to involve the enhancement of store-operated Ca^{2+} influx only, including both TRPCs channels.

Potential clinical implications. Our present study together with the aforementioned recent one (10) reveals new, previously unanticipated clinical effects for α_1-AR blockade in the control of prostate epithelial cell proliferation, which can be further exploited for growth suppression in the benign and malignant prostate. Moreover, because we have identified the signaling pathway mediating α_1-AR–stimulated proliferation promotion, all the molecular entities involved can potentially represent suitable targets for therapeutic intervention. This is especially true with respect to the TRPC6 channel, which determines the oscillatory pattern of Ca^{2+} signaling that couples agonist-mediated α_1-AR stimulation to Ca^{2+}-dependent activation of the NFAT transcription factor, as disrupting this pattern would ultimately terminate proliferative gene expression.

Acknowledgments

Received 2/3/2005; revised 11/25/2005; accepted 12/21/2005.

Grant support: Institut National de la Sante et de la Recherche Medicale, Ligue Nationale Contre le Cancer, Association pour la Recherche Contre le Cancer, and Ministère de l'Education Nationale, France (Y. Shuba).

The costs of publication of this article were defrayed in part by the payment of page charges. This article must therefore be hereby marked *advertisement* in accordance with 18 U.S.C. Section 1734 solely to indicate this fact.

We thank Etienne Dewailly and Philippe Delcourt for technical support.

References

1. Berridge MJ, Bootman MD, Lipp P. Calcium: a life and death signal. Nature 1998;395:645–8.
2. Clapham DE. Calcium signaling. Cell 1995;80:259–68.
3. Patterson RL, van Rossum DB, Ford DL, et al. Phospholipase C-gamma is required for agonist-induced Ca^{2+} entry. Cell 2002;111:529–41.
4. Putney JW, Jr., Broad LM, Braun FJ, Lievremont JP, Bird GS. Mechanisms of capacitative calcium entry. J Cell Sci 2001;114:2223–9.
5. Caine M. Alpha-adrenergic blockers for the treatment of benign prostatic hyperplasia. Urol Clin North Am 1990;17:641–9.
6. Kyprianou N, Chon J, Benning CM. Effects of alpha(1)-adrenoceptor (alpha(1)-AR) antagonists on cell proliferation and apoptosis in the prostate: therapeutic implications in prostatic disease. Prostate Suppl 2000; 9:42–6.
7. Kyprianou N, Benning CM. Suppression of human prostate cancer cell growth by alpha1-adrenoceptor antagonists doxazosin and terazosin via induction of apoptosis. Cancer Res 2000;60:4550–5.
8. Benning CM, Kyprianou N. Quinazoline-derived alpha1-adrenoceptor antagonists induce prostate cancer cell apoptosis via an alpha1-adrenoceptor-independent action. Cancer Res 2002;62:597–602.
9. Horoszewicz JS, Leong SS, Kawinski E, et al. LNCaP model of human prostatic carcinoma. Cancer Res 1983; 43:1809–18.
10. Thebault S, Roudbaraki M, Sydorenko V, et al. Alpha1-adrenergic receptors activate Ca(2+)-permeable cationic channels in prostate cancer epithelial cells. J Clin Invest 2003;111:1691–701.
11. Vanoverberghe K, Mariot P, Vanden Abeele F, Delcourt P, Parys JB, Prevarskaya N. Mechanisms of ATP-induced calcium signaling and growth arrest in human prostate cancer cells. Cell Calcium 2003;34: 75–85.
12. Minneman KP. Alpha 1-adrenergic receptor subtypes, inositol phosphates, and sources of cell Ca^{2+}. Pharmacol Rev 1988;40:87–119.
13. Marshall I, Burt RP, Chapple CR. Signal transduction pathways associated with alpha1-adrenoceptor subtypes in cells and tissues including human prostate. Eur Urol 1999;36:42–7; discussion 65.
14. Clapham DE. TRP channels as cellular sensors. Nature 2003;426:517–24.
15. Golovina VA. Cell proliferation is associated with enhanced capacitative Ca(2+) entry in human arterial myocytes. Am J Physiol 1999;277:C343–9.
16. Golovina VA, Platoshyn O, Bailey CL, et al. Upregulated TRP and enhanced capacitative Ca(2+) entry in human pulmonary artery myocytes during proliferation. Am J Physiol Heart Circ Physiol 2001; 280:H746–55.
17. Inoue R, Okada T, Onoue H, et al. The transient receptor potential protein homologue TRP6 is the essential component of vascular alpha(1)-adrenoceptor-activated Ca(2+)- permeable cation channel. Circ Res 2001;88:325–32.
18. Montell C. Physiology, phylogeny, and functions of the TRP superfamily of cation channels. Sci STKE 2001; 2001:RE1.
19. Crabtree GR. Calcium, calcineurin, and the control of transcription. J Biol Chem 2001;276:2313–6.
20. Li X, Stark GR. NFkappaB-dependent signaling pathways. Exp Hematol 2002;30:285–96.
21. van Leenders GJ, Aalders TW, Hulsbergen-van de Kaa CA, Ruiter DJ, Schalken JA. Expression of basal cell keratins in human prostate cancer metastases and cell lines. J Pathol 2001;195:563–70.
22. Grynkiewicz G, Poenie M, Tsien RY. A new generation of Ca^{2+} indicators with greatly improved fluorescence properties. J Biol Chem 1985;260:3440–50.
23. Skryma R, Mariot P, Bourhis XL, et al. Store depletion and store-operated Ca^{2+} current in human prostate cancer LNCaP cells: involvement in apoptosis. J Physiol 2000;527 Pt 1:71–83.
24. Skryma RN, Prevarskaya NB, Dufy-Barbe L, Odessa MF, Audin J, Dufy B. Potassium conductance in the androgen-sensitive prostate cancer cell line, LNCaP: involvement in cell proliferation. Prostate 1997;33: 112–22.
25. Vanden Abeele F, Skryma R, Shuba Y, et al. Bcl-2-dependent modulation of Ca(2+) homeostasis and store-operated channels in prostate cancer cells. Cancer Cell 2002;1:169–79.
26. Vanden Abeele F, Roudbaraki M, Shuba Y, Skryma R, Prevarskaya N. Store-operated Ca^{2+} current in prostate cancer epithelial cells. Role of endogenous Ca^{2+} transporter type 1. J Biol Chem 2003;278: 15381–9.
27. Sydorenko V, Shuba Y, Thebault S, et al. Receptor-coupled, DAG-gated Ca^{2+}-permeable cationic channels in LNCaP human prostate cancer epithelial cells. J Physiol 2003;548:823–36.
28. Fang WG, Pirnia F, Bang YJ, Myers CE, Trepel JB. P2-purinergic receptor agonists inhibit the growth of androgen-independent prostate carcinoma cells. J Clin Invest 1992;89:191–6.
29. Thebault S, Zholos A, Enfissi A, et al. Receptor-operated Ca(2+) entry mediated by TRPC3/TRPC6 proteins in rat prostate smooth muscle (PS1) cell line. J Cell Physiol 2005;204:320–8.
30. Vanden Abeele F, Lemonnier L, Thebault S, et al. Two types of store-operated Ca^{2+} channels with different activation modes and molecular origin in LNCaP human prostate cancer epithelial cells. J Biol Chem 2004;279: 30326–37.
31. Sotillo R, Renner O, Dubus P, et al. Cooperation between Cdk4 and p27kip1 in tumor development: a preclinical model to evaluate cell cycle inhibitors with therapeutic activity. Cancer Res 2005;65:3846–52.
32. Pattni K, Millard TH, Banting G. Calpain cleavage of the B isoform of Ins(1,4,5)P3 3-kinase separates the catalytic domain from the membrane anchoring domain. Biochem J 2003;375:643–51.
33. Sims CE, Allbritton NL. Metabolism of inositol 1,4,5-trisphosphate and inositol 1,3,4,5-tetrakisphosphate by the oocytes of *Xenopus laevis*. J Biol Chem 1998;273: 4052–8.
34. Allbritton NL, Meyer T, Stryer L. Range of messenger action of calcium ion and inositol 1,4,5-trisphosphate. Science 1992;258:1812–5.
35. Wang SS, Alousi AA, Thompson SH. The lifetime of inositol 1,4,5-trisphosphate in single cells. J Gen Physiol 1995;105:149–71.
36. Fujii R, Imahori Y, Ido T, et al. [Carbon-11 labeled diacylglycerol for signal transduction imaging by positron CT: evaluation of the quality and safety for clinical use]. Kaku Igaku 1995;32:191–8.
37. Dolmetsch RE, Xu K, Lewis RS. Calcium oscillations increase the efficiency and specificity of gene expression. Nature 1998;392:933–6.
38. Mignen O, Thompson JL, Shuttleworth TJ. Calcineurin directs the reciprocal regulation of calcium entry pathways in nonexcitable cells. J Biol Chem 2003;278: 40088–96.
39. Mignen O, Thompson JL, Shuttleworth TJ. Reciprocal regulation of capacitative and arachidonate-regulated noncapacitative Ca^{2+} entry pathways. J Biol Chem 2001; 276:35676–83.
40. Beech DJ, Xu SZ, McHugh D, Flemming R. TRPC1 store-operated cationic channel subunit. Cell Calcium 2003;33:433–40.
41. Plant TD, Schaefer M. TRPC4 and TRPC5: receptor-operated Ca^{2+}-permeable nonselective cation channels. Cell Calcium 2003;33:441–50.
42. Trebak M, Bird GS, McKay RR, Birnbaumer L, Putney JW, Jr. Signaling mechanism for receptor-activated TRPC3 channels. J Biol Chem 2003;278:16244–52.
43. Hofmann T, Obukhov AG, Schaefer M, Harteneck C, Gudermann T, Schultz G. Direct activation of human TRPC6 and TRPC3 channels by diacylglycerol. Nature 1999;397:259–63.
44. Estacion M, Li S, Sinkins WG, et al. Activation of human TRPC6 channels by receptor stimulation. J Biol Chem 2004;279:22047–56.
45. Sweeney M, Yu Y, Platoshyn O, Zhang S, McDaniel SS, Yuan JX. Inhibition of endogenous TRP1 decreases capacitative Ca^{2+} entry and attenuates pulmonary artery smooth muscle cell proliferation. Am J Physiol Lung Cell Mol Physiol 2002;283:L144–55.
46. Yu Y, Sweeney M, Zhang S, et al. PDGF stimulates pulmonary vascular smooth muscle cell proliferation by upregulating TRPC6 expression. Am J Physiol Cell Physiol 2003;284:C316–30.